PROCEEDINGS OF SCIENCE

Search for VHE gamma-ray emission from Geminga pulsar and Nebula with the MAGIC telescopes

Simon Bonnefoy*, Marcos Lopez*, Ruben Lopez-Coto⋆,Takayuki Saito† For the MAGIC Collaboration.

*Authors affiliation: *Universidad Complutense de Madrid, E28040 Madrid, Spain, ⋆IFAE, Campus UAB, E-08193 Bellaterra, Spain, †Kyoto University, Japan*

E-mail: simon@gae.ucm.es, marcos@gae.ucm.es, rlopez@ifae.es, tysaito@cr.scphys.kyoto-u.ac.jp

The Geminga pulsar appears to be one of the most promising candidates to detect very high energy (VHE > 100 GeV) gamma-ray pulsed emission. In order to find a second pulsar at hundreds of GeVs in the northern sky, we analyzed 63 hours of data. To discuss the connection with HE gamma rays, 6 years of *Fermi*-LAT data were also analyzed. No significant pulsed emission was found in the MAGIC data. The obtained flux upper limits at 50 GeV lie above the power law extrapolation above 10 GeV from *Fermi*-LAT data. A search for steady emission from the pulsar wind nebula in the same dataset similarly led to no significant detection.

The 34th International Cosmic Ray Conference,
30 July- 6 August, 2015
The Hague, The Netherlands

PoS(ICRC2015)738

1. Introduction

Geminga is the prototype of the radio quiet pulsar, the second brightest persistent source in the GeV sky and the closest γ-ray object of this type ($d \sim 250$ pc) ([1]). Its light curve exhibits two peaks, hereafter P1 and P2, separated by 0.5 in phase. Emission from bridge, i.e., between P1 and P2, has been reported ([2]). The period of Geminga ($P \sim 237$ ms) ([3]) and its derivative ($\dot{P} \sim 1.1 \times 10^{-14}$ s/s) correspond to a spin-down age of $\tau \sim 340$ kyr, a spin-down power $\dot{E}_{\rm rot} = 3.3 \times 10^{34}$ erg s^{-1} and a surface magnetic field $B_{\rm surf} \sim 1.6 \times 10^{12}$ G. Although its spin-down luminosity itself is not as high as those of Crab and Vela, the short distance to this source makes its spin-down flux very large, which implies a high gamma-ray flux.

The Geminga pulsar, with one of the highest flux detected in the gamma-ray band ([4]), is a good candidate to emit gamma-rays in the energy range reachable by Cherenkov telescopes. Its timing and spectral measurements can shed light on the location and emission mechanism at work in such an old pulsar. The first Geminga spectrum was computed by using the *EGRET* telescope, on-board of the *Compton Gamma-Ray Observatory* and is well described by a power-law from 30 MeV to 2 GeV ([5]). Observations at high energies with *Fermi*-LAT including one year of data reported a power-law with an exponential cut-off at (2.5 ± 0.2) GeV ([6]). The pulsation is still clearly seen above 10 GeV with a reported significance greater than 6 σ ([7]). The presence of a signal above 25 GeV is also confirmed (with a *p-value* < 0.05 in this energy range). Recently VERITAS reported about the search for very high energy (VHE) emission from the Geminga pulsar with no signal detected above 100 GeV ([8]). They computed flux integral upper limits of $4.0 \times 10^{-13}[s^{-1}cm^{-2}]$ and $1.7 \times 10^{-13}[s^{-1}cm^{-2}]$ above 135 GeV for P1 and P2, respectively.

Besides the emission from the pulsar, an X-ray nebula was discovered around the Geminga pulsar by the XMM-Newton and Chandra satellites ([9], [10]). Both detections showed the presence of an extended structure behind the pulsar, aligned with the latter's proper motion direction. In gamma-rays, the *Fermi*-LAT reported the detection of an emission over the whole pulsar rotation, but that is incompatible with a surrounding nebula ([6]).

However, the Milagro collaboration reported the detection of a extended, steady TeV gamma-ray emission from Geminga at a significance level of 6.3σ. They observed an extended emission region 2-3 degrees across that emits a flux at 35 TeV of $(38 \pm 11) \times 10^{-17}$ TeV^{-1} cm^{-2} s^{-1} ([11]).

2. MAGIC observations and data analysis

The MAGIC telescopes are a set of two 17-meters diameter imaging atmospheric Cherenkov telescopes, designed to detect gamma-rays above 50 GeV. The trigger threshold for standard observations at zenithal angles below 35° is around 50 GeV

Observations of the Geminga pulsar and nebula were performed between December 2012 and March 2013, with the upgraded MAGIC telescopes ([12]). During this period, a total of $\sim$ 75 hours were taken at zenith angles below 35°, to assure the lowest possible energy threshold. The observations were performed in the so-called wobble mode ([13]), where the source is offset 0.4° from the camera center.

The data analysis was proceeded using the standard MAGIC analysis chain *MARS* ([14]). The phasing of the events was computed using *tempo2* ([15]). The ephemeris was provided by the *Fermi*-

LAT collaboration[1]. For the pulsed analysis, the cuts are computed using a background sample and Monte Carlo data by maximizing in each energy bin the Q-factor defined as: $Q = \varepsilon_{on}/\sqrt{\varepsilon_{off}}$, where ε_{on} and ε_{off} are the cuts efficiency for on and off data, respectively. The maximization was done scanning over the *hadronness*, a parameter that characterizes whether an event is more likely to be a proton or a gamma, and θ^2 which is the squared angular distance between the source position and the reconstructed source position in the camera.

The upper limits for both pulsed and steady emission were computed using the Rolke method ([16]) assuming a Poissonian background and requiring a 95% confidence level. The search for a steady extended emission was done computing the signal to noise ratio around the Geminga pulsar. Several extensions around the Geminga pulsar were considered, setting the value of the cut in θ^2 (0.04, 0.06, 0.08 and 0.1 deg^2). Also, a sky map of the region around the Geminga pulsar was produced. The differential upper limits for the nebula emission were computed assuming a spectral index of -2.6.

3. Fermi-LAT

3.1 Fermi data analysis

A data sample of 6 years (from 2008-09-01 to 2014-11-18) of *Fermi*-LAT data was analysed in order to compute the peaks position at high energy and extrapolate a possible emission at VHE. The high-energy radiation was fit to a power-law function, above 10 GeV, and extrapolated up to 100 GeV. We analysed this data-set using the PASS7 instrument response functions and the *Fermi* tools version v9r31p1.

3.2 Fermi-LAT results

To estimate the pulse profiles we used photons with energies greater than 5 GeV and 10 GeV for P1 and P2, respectively. We take the highest possible energy in order to have peak widths that are more consistent with the ones we would expect at MAGIC energies, and, at the same time, to have enough statistics. The SEDs of P1, P2 and phase averaged were computed assuming a power-law with a sub-exponential cut-off function, defined as:

$$\frac{dF}{dE} = N_0 \left(\frac{E}{E_0}\right)^{-\alpha} exp(-(E/E_c)^b), \tag{3.1}$$

where E_0 is the energy scale set as 510.7 GeV as computed in ([17]), α the spectral index, and E_c the energy cut-off and $b < 1$ for a sub-exponential cut-off. We also fit the *Fermi*-LAT data above 10 GeV using a power-law function. The resulting fit parameters are shown in Table 1

4. MAGIC Results

The results of the timing analysis of MAGIC data are shown in Fig. 1. We computed the light curve and corresponding significances for the pulsed emission in several energy ranges; above 50

[1]http://www.slac.stanford.edu/∼kerrm/fermi_pulsar_timing/J0633+1746/html/J0633+1746_54683_56587_chol.par

	N_0	α
P1	$(1.5 \pm 0.3) \times 10^{-15}$	-5.7 ± 0.2
P2	$(1.3 \pm 0.2) \times 10^{-14}$	-5.4 ± 0.2

Table 1: Results of the likelihood fit of P1 and P2 spectral energy distribution to a power law above 10 GeV. The normalization factor is given in units of [MeV^{-1} s^{-1} cm^{-2}].

GeV, 50-100 GeV and 100-200 GeV. We evaluated the significance of the pulsed signal in the regions defined as P1 (phase 0.066 to 0.118) and P2 (phase 0.565 to 0.607). The background is estimated from the off-region (phase 0.70 to 0.95). We computed the significance for P1, P2, and the sum of both peaks. The results of the statistical tests are shown in Table 2. No significant pulsation was found in MAGIC data in any of the energy ranges investigated. The upper limits computed for the pulsed emission are shown in Figure 2 with blue arrows. In Figure 2 the blue lines on top of the arrows represent the spectral slope assumed for the upper limits computation, the dot-dot-dashed blue lines represent the fit of *Fermi*-LAT data above 10 GeV to a power-law function, and the butterfly plot for the power-law fit at high energy, that represents the statistical error contours.

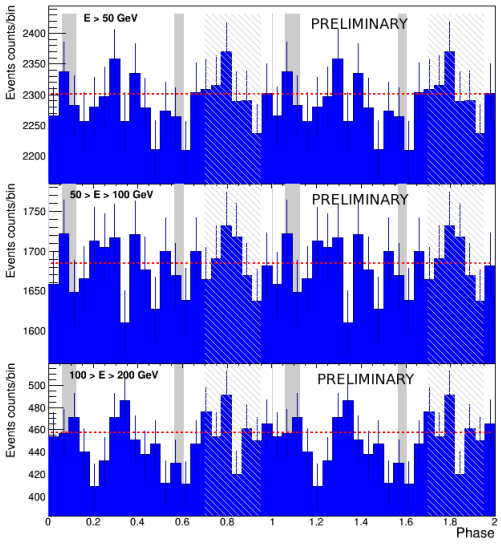

Figure 1: Light curves of the Geminga pulsar obtained with MAGIC for different energy bins. From top to bottom: above 50 GeV, 50-100GeV and 100-200 GeV. Two cycles are plotted for clarity. The shaded areas show the position of P1 (main pulse) and P2 (interpulse). The white area shows the off-region. The dashed red line represents the averaged number of events in the background region.

Figure 3 shows the MAGIC sky map computed around Geminga. The position of the Geminga pulsar is marked by a cross. The white circle shows the PSF after smearing the sky map using a Gaussian Kernel. No significant emission was found from the Geminga nebula above 50 GeV. We calculated the upper limits for the nebula's differential emission in the energy range covered by MAGIC. These limits ar represented by blue arrows in Figure 4. The computed phase-averaged SED of the Geminga pulsar, using 6 years of *Fermi*-LAT data, is represented by the black points.

Energy range (GeV)	P1	P2	P12
≥ 50	0.2σ	-0.1σ	0.1σ
50-100	-0.2σ	-0.2σ	0.0σ
100-200	0.7σ	-1.4σ	-0.3σ

Table 2: Significances evaluated for the two, P1 and P2, peaks regions.

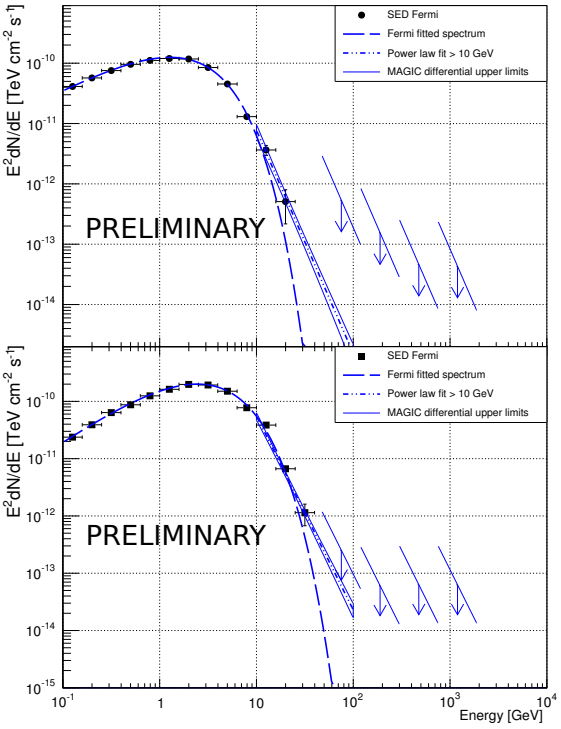

Figure 2: SED for P1 (top) and P2 (bottom). The differential upper limits are represented by the blue arrows. The blue dashed lines represent the SED computed using 6 years of *Fermi*-LAT data. The dot-dot-dashed lines represent the fit of the *Fermi* data above 10 GeV with a power-law.

The dashed blue lines are the result of *Fermi* spectral shape computation using a power-law with a sub-exponential cut-off function. The green point represents the flux level of the Geminga nebula as seen by MILAGRO ([11]).

5. Discussion and conclusions

During the winter 2012/13, the Geminga pulsar and its surrounding nebula were observed for 63 hours by the MAGIC telescopes. The analysis of the MAGIC data has returned in upper limits above 50 GeV for both pulsed and steady emission. The computed upper limits for the pulsed flux are higher than the power-law extrapolation of the *Fermii*-LAT above 10 GeV. Beside MAGIC data, 6 years of *Fermi*-LAT data were analyzed to derive pulsed and phase averaged emission. The SEDs computed using the *Fermi*-LAT data are represented by a power-law with a sub-exponential cut-off. As reported by Lyutikov ([19]), a simple power-law could also characterize the spectral points at

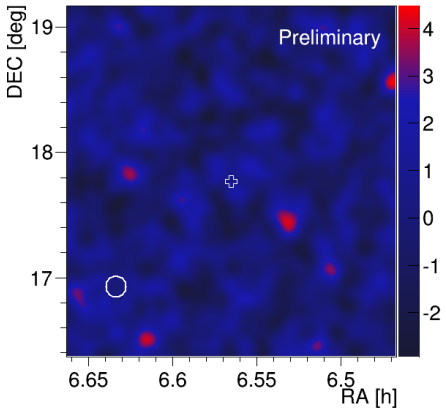

Figure 3: MAGIC Sky map computed above 50 GeV around the location of the Geminga pulsar. The cross at the center of the map represents the Geminga pulsar location. The white circle represents the function used for the deconvolution of the sky map. The z-axis represents the significance.

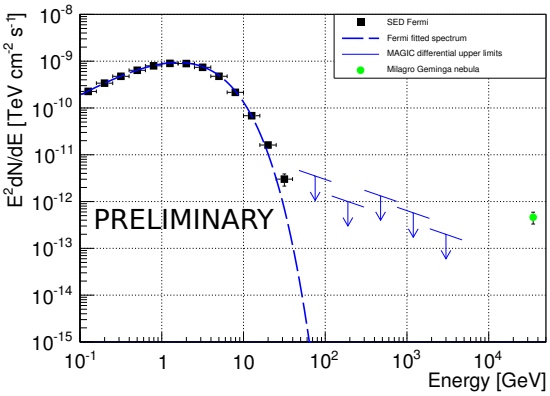

Figure 4: Phase averaged SED. The differential upper limits of the Geminga nebula computed using the MAGIC data are represented by the blue arrows. The blue dashed line represents the phase average SED of the Geminga pulsar computed using 6 years of *Fermi*-LAT data. The green point is the flux level of the extended steady emission from Geminga seen by MILAGRO.

high energy, but more statistics would be required to disentangle between these two spectral shapes. Two mechanims are expected to be responsible of the pulsars high energy emission; the synchro-curvature radiation and the inverse Compton scattering. Synchro-curvature radiation would exhibit an exponential or sub-exponential cut-off at few GeVs ([20], [21]) , and a power-law tail would strongly disfavour synchro-curvature radiation ([22]) before inverse Compton scattering. A hard gamma-ray tail is not expected even if the curvature radiation is produced in a curved magnetic field close to the light cylinder ([23]). The MAGIC upper limits, being at a higher flux level than the *Fermi*-LAT extrapolation, cannot constrain the spectral shape at high energy.

The analysis of the MAGIC data for Geminga nebula shows no significant detection at MAGIC energies. The presence of the nebula is unknown at the GeV scale. Indeed, the observation of the Geminga pulsar with the *Fermi*-LAT shows no evidence of a surrounding nebula. The detection,

with MAGIC, of a large nebula similar to the one claimed by Milagro is not straightforward since its extension exceeds MAGIC's field of view. However, the upcoming Cherenkov Telescope Array (CTA) ([24]) with higher sensitivity and lower energy threshold than the current Cherenkov telescopes could eventually detect high energy emission from the Geminga pulsar and shed light physics at work in such an old pulsar.

6. Acknowledgements

We would like to thank the Instituto de Astrofísica de Canarias for the excellent working conditions at the Observatorio del Roque de los Muchachos in La Palma. The support of the German BMBF and MPG, the Italian INFN, the Swiss National Fund SNF, and the ERDF funds under the Spanish MICINN is gratefully acknowledged. This work was also supported by the CPAN CSD2007-00042 and MultiDark CSD2009-00064 projects of the Spanish Consolider-Ingenio 2010 programme, by grant 268740 of the Academy of Finland, by the Croatian Science Foundation (HrZZ) Project 09/176, by the DFG Collaborative Research Centers SFB823/C4 and SFB876/C3, by the Polish MNiSzW grant 745/N-HESS-MAGIC/2010/0 and by the Ramón y Cajal program from the Spanish MICINN.

References

[1] Halpern, J. P. and Ruderman, M., ApJ **415** (1992) 286-297,

[2] Fierro, J. M. and Michelson, P. F. and Nolan, P. L. and Thompson, D. J., ApJ **494** (1998) 734-746,

[3] Halpern, J. P. and Holt, S. S., Nature, 357 (1992) 222-224,

[4] The Fermi-LAT Collaboration, arXiv, 1501.02003, (2015)

[5] Mayer-Hasselwander, H. A. et al. ApJ **421** (1994) 276-283

[6] Abdo, A. A. et al. ApJ **720** (2010) 272-283

[7] Ackermann, M. et al. arXiv, 1306.6772, (2013)

[8] Aliu, E. et al.ApJ **800** (2015) 61

[9] de Luca, A. and Caraveo, P. A. and Mattana, F. and Pellizzoni, A. and Bignami, G. F., A&A **445** (2006) L9-L13

[10] Pavlov, G. G. and Bhattacharyya, S. and Zavlin, V. E., ApJ **715** (2010) 66-77

[11] Abdo, A. A. et al. ApJ, **700** (2009) L127-L131

[12] Aleksic, J. et al. ArXiv e-prints 1409.6073, (2014)

[13] Fomin, V. P. and Stepanian, A. A. and Lamb, R. C. and , Lewis, D. A. and Punch, M. and Weekes, T. C., Astroparticle Physics, **2** (1994) 137-150

[14] Zanin, R. et al. Proceeding of the 33rd ICRC, Rio de Janeiro, (2013)

[15] Hobbs, G. B. and Edwards, R. T. and Manchester, R. N., , astro-ph/0603381, (2006)

[16] Rolke, W. A. and López, A. M., Nuclear Instruments and Methods in Physics Research A, **458** (2001) 745-758

[17] Nolan, P. L. et al. ApJ **199** (2012) 31

[18] Albert, J. et al. ApJ **35** (2008) 1070-1073

[19] Lyutikov, M.,ApJ **757** (2012) 88

[20] Prosekin, A. Y. and Kelner, S. R. and Aharonian, F. A.,ArXiv e-prints 1305.0783, (2013)

[21] Viganò, D. and Torres, D. F., MNRAS, **449** 3755-3765, (2015)

[22] Lyutikov, M. and Otte, N. and McCann, A.,ApJ **754** (2012) 33,

[23] Bednarek, W., MNRAS, **424** 2079-2085, (2012)

[24] Bernlöhr, K. and others arXiv, 1210.3503 (2013)